© 2017. Published by The Company of Biologists Ltd | Journal of Experimental Biology (2017) 220, 705-712 doi:10.1242/jeb.148767

RESEARCH ARTICLE

Batoid locomotion: effects of speed on pectoral fin deformation in the little skate, *Leucoraja erinacea*

Valentina Di Santo[1,*], Erin L. Blevins[1,2] and George V. Lauder[1]

ABSTRACT

Most batoids have a unique swimming mode in which thrust is generated by either oscillating or undulating expanded pectoral fins that form a disc. Only one previous study of the freshwater stingray has quantified three-dimensional motions of the wing, and no comparable data are available for marine batoid species that may differ considerably in their mode of locomotion. Here, we investigate three-dimensional kinematics of the pectoral wing of the little skate, *Leucoraja erinacea*, swimming steadily at two speeds [1 and 2 body lengths (BL) s^{-1}]. We measured the motion of nine points in three dimensions during wing oscillation and determined that there are significant differences in movement amplitude among wing locations, as well as significant differences as speed increases in body angle, wing beat frequency and speed of the traveling wave on the wing. In addition, we analyzed differences in wing curvature with swimming speed. At 1 BL s^{-1}, the pectoral wing is convex in shape during the downstroke along the medio-lateral fin midline, but at 2 BL s^{-1} the pectoral fin at this location cups into the flow, indicating active curvature control and fin stiffening. Wing kinematics of the little skate differed considerably from previous work on the freshwater stingray, which does not show active cupping of the whole fin on the downstroke.

KEY WORDS: Fin stiffness, Pectoral fin, Elasmobranch, Swimming performance, Kinematics

INTRODUCTION

Batoids (rays, skates, guitarfishes and sawfishes) are cartilaginous fishes characterized by dorso-ventrally flattened bodies, with expanded pectoral fins fused to the cranium that form a disc ranging in shape from round to rhomboidal (Aschliman et al., 2012; Franklin et al., 2014; Nakamura et al., 2015). Most rays and all skates use their pectoral fins to swim and can be placed into a continuum between undulatory and oscillatory, based on the number of kinematic waves present on the wing during steady locomotion (Rosenberger, 2001). Undulatory (or rajiform) locomotion is often observed in benthic species and is defined by having more than one propulsive wave present on the fin at one time, while oscillatory (or mobuliform) locomotion is most commonly observed in pelagic species and is defined by having less than a half wave present on the flapping pectoral fin disc (Rosenberger, 2001; Schaefer and Summers, 2005). The rajiform mode is specialized for efficient swimming at low speeds, because of high stability and maneuverability, while the mobuliform locomotion is considered more efficient at higher speeds and for long-distance translocations (Di Santo and Kenaley, 2016). Although many batoid species are accurately described by these two extreme modes, several species fall into a continuum between 0.5 and 1.0 wave, and are defined as 'semi-oscillators' (Schaefer and Summers, 2005).

The mechanics of propulsion in cartilaginous fishes have been investigated over the years through studies of morphology, kinematics, hydrodynamics, muscle activity and energetics (Daniel, 1988; Di Santo and Kenaley, 2016; Donley and Shadwick, 2003; Fontanella et al., 2013; Lauder, 2015; Lauder and Di Santo, 2015; Porter et al., 2011; Rosenberger and Westneat, 1999; Rosenblum et al., 2011). Most of the work on live animals has focused on sharks rather than batoids, perhaps owing to the fact that pelagic rays are generally difficult to maintain in laboratory settings and smaller benthic batoids often prefer to 'punt' (or walk) on the substrate rather than swim in the water column (Koester and Spirito, 2003; Macesic and Kajiura, 2010; Macesic and Summers, 2012; Macesic et al., 2013), making studies of free-swimming challenging to conduct. To date, only a few studies have attempted to quantify swimming kinematics of batoids (e.g. Fish et al., 2016; Fontanella et al., 2013; Parson et al., 2011; Rosenblum et al., 2011), and three-dimensional deformation of the wing during swimming has only been described in one species, the freshwater stingray, *Potamotrygon orbignyi* (Blevins and Lauder, 2012). Although the extreme morphology of batoids renders the wing disc essentially two-dimensional in shape, the disc assumes a complex three-dimensional conformation during swimming that can be effectively described only using three-dimensional kinematic analyses (Blevins and Lauder, 2012; Lauder and Jayne, 1996).

In this study, we examine the three-dimensional kinematics of the pectoral fin of the little skate, *Leucoraja erinacea* (Mitchill 1825), during steady swimming. The little skate is known to have the lowest swimming metabolic rate measured in any elasmobranch at its optimal cruising speed (~1 BL s^{-1}, where BL is body lengths) (Di Santo and Kenaley, 2016), with an energetic cost of locomotion similar to that of one of the most efficient migratory fishes, the European eel, *Anguilla anguilla* (van Ginneken et al., 2005). Di Santo and Kenaley (2016) have reported that little skates are unable to sustain speeds beyond their optimal speed for more than a few minutes, suggesting their swimming is confined to the descending portion of the metabolic rate–speed relationship.

We focused this paper on three-dimensional wing kinematics of the little skate for four reasons. First, kinematic data are an important adjunct to a previous metabolic study (Di Santo and Kenaley, 2016) which quantified the cost of transport in this species over a range of swimming speeds similar to those used in the present study. The availability of correlated analyses of metabolic and detailed kinematic data are rare for any fish species, and observed changes in patterns of wing deformation with swimming speed may help explain previous data showing the inability of this fish to sustain swimming at higher speeds (>1.25 BL s^{-1}) for more than a few

[1]Museum of Comparative Zoology, Harvard University, Cambridge, MA 02138, USA. [2]The Winsor School, Boston, MA 02215, USA.

*Author for correspondence (vdisanto@fas.harvard.edu)

V.D., 0000-0002-5419-3747

Received 23 August 2016; Accepted 4 December 2016

Journal of Experimental Biology (2017) 220, 705-712 doi:10.1242/jeb.148767

minutes. Second, three-dimensional kinematic data are only available for one other batoid species, the specialized freshwater stingray (Blevins and Lauder, 2012). A secondary purpose of this paper is to provide comparative data to allow at least a preliminary assessment of the diversity of batoid wing kinematics in non-pelagic species. Third, batoids are increasingly serving as subjects for robotic models of aquatic propulsion (e.g. Blevins and Lauder, 2013; Cloitre et al., 2012; Dewey et al., 2012; Krishnamurthy et al., 2010; Moored et al., 2011a,b; Park et al., 2016), and yet three-dimensional biological data on how the wing moves are extremely limited. Such data are needed to provide a template for programming robotic ray wing surface motions, and we aim to provide a new kinematic data set on wing-based aquatic propulsion for this purpose. Fourth, active stiffening of tissues as speed changes is a key area of interest in aquatic locomotion. For fishes, activation of red musculature along the body causes changes in stiffness and the fluid–structure interaction that may be related to changing locomotor efficiency (Flammang, 2010; Long et al., 2011; Root et al., 2007; Tytell et al., 2010, 2014), but data suggesting active changes in wing surface stiffness are not available for any batoid. By analyzing wing kinematics over a doubling of swimming speed in the little skate, we aim to determine whether kinematic data show evidence of active wing stiffening by intrinsic musculature. Data presented below reveal substantial differences in wing kinematics between the little skate and previous work on the freshwater stingray, and provide evidence for active stiffening of the wing surface at the highest velocity that may explain the possibly prohibitive metabolic costs of prolonged swimming beyond an optimal cruising speed (Di Santo and Kenaley, 2016).

MATERIALS AND METHODS

Animals and experimental setup

Little skates (*L. erinacea*) were obtained from the Marine Biological Laboratory (Woods Hole, MA, USA) and transported to the Museum of Comparative Zoology Laboratories at Harvard University. Juvenile skates (n=3), ranging in size from 6.6 to 8.5 cm (disc length, DL) and from 18.2 to 35.1 g, were maintained in a 1500-liter recirculating tank at 14°C, 33 ppt salinity and 8.1 pH under a 12 h:12 h light:dark photoperiod. Skates were fed a diet of frozen mysid shrimp (Piscine Mysis®) *ad libitum* daily, but were fasted for 24 h prior to each swimming trial. All experiments were performed according to the approved Harvard University IACUC protocol (no. 20-03).

Morphology

Three-dimensional pectoral fin morphology was studied to determine the pattern of pectoral disc thickness and to aid in the interpretation of kinematic data. A three-dimensional model of the left pectoral fin of a little skate (5.5 cm DL) was reconstructed from micro-CT analysis (Fig. 1A–C). The pectoral fin of the specimen was scanned at 58 µA and 90 kV for 250 ms with a rotation angle of 0.7 deg (SkyScan1173, Micro Photonics, Inc., Allentown, PA, USA). The images produced had a voxel size of 71 µm. Slices were reconstructed in NRecon (Micro Photonics, Inc.) and then exported into Mimics 15.0 (Materialise, Leuven, Belgium) for analysis of thickness. Each coronal slice was analyzed in ImageJ (National Institutes of Health, Bethesda, MD, USA) and thickness was measured for each sagittal slice to obtain thickness across the skate pectoral fin (Fig. 1C).

Swimming protocol and kinematic analyses

Little skates were recorded (Movie 1) while swimming at two speeds (1 and 2 BL s^{-1}, body length defined as DL) in a flow tank with a total working section of 28×28×66 cm as in previous work (see Tytell and Lauder, 2004), at a constant temperature (14±1°C) and salinity (33 ppt), at a Reynolds number of approximately 10,000 (based on DL). We placed a 20 deg angled baffle in the working section to prevent the skates from resting on the bottom of the tank and only recorded sequences where fish were swimming in the center of the tank and away from all walls and the baffle. Lateral and dorsal views of steady swimming at two speeds were recorded by two synchronized 1-megapixel high-speed video cameras (FASTCAM 1024 PCI; Photron USA, San Diego, CA, USA) at 250 frames s^{-1}. The dorsal view was recorded using a 45 deg mirror above the swim tunnel, and a floating Plexiglas® panel at the water surface prevented surface ripples from interfering with dorsal view videos. Videos from the two cameras were calibrated and aligned to recreate the images in three-dimensional space using direct linear transformation in MATLAB (MathWorks, Natick, MA, USA) and using a calibration program (Hedrick, 2008).

We digitized nine points on the left pectoral wing of the skates (Fig. 2) during three independent (non-consecutive) fin beats (or swimming sequences) from each of the three individuals at the two speeds every 20 ms (total finbeats=18). Fin beats were defined as a complete cycle of disc wave, from the anterior to the posterior edge (Blevins and Lauder, 2012). We used natural markings on the dorsal surface of each skate left wing to track the nine points and determine the 3D deformation of the wing by analyzing the x, y and z coordinates of each point in time. Although each skate varies slightly in the location of natural markers that define the locations that we wished to digitize, the marked points were within 1 mm of each other among the different individual skates. We prefer marked points even at the cost of increasing variation among individuals because digitizing natural marks reduces intra-individual variation; we have previously used natural markings in studies of freshwater stingray and leopard shark locomotion (Blevins and Lauder, 2012; Wilga and Lauder, 2002).

These points were chosen to describe the contour of the pectoral fin as follows (Fig. 2). Point 1 is the most anterior tip of rostrum. Point 9 is the postero-medial extreme of the pectoral fin, specifically not including the pelvic fin, which extends further posteriorly. This point is identified by its location just lateral to the body midline, where the pectoral fin meets the body and by a small natural marking that is present in some individuals. Points 3, 4 and 8 are equidistant from anterior to posterior along the fin margin, with point 4 located at the most lateral point on the wing. Points 3 and 8 may have natural pigmented markings associated with their locations in some individuals. Points 5, 6 and 7 are equidistant and divide the wing from distal to proximal in nearly equal distances from point 4 to point 7 at a marking just lateral to the body midline. Point 2 marks the middle of the eye ridge as seen in dorsal view where a small lateral projection occurs (Fig. 2).

We calculated mean values for amplitude, frequency, wavespeed, whole-body angle of attack, and spanwise and chordwise fin curvature (also see Blevins and Lauder, 2012). These kinematic variables were used to characterize the deformation of the fin during locomotion and differences between the two speeds. Briefly, maximum amplitude (mm) was calculated at each digitized point on the fin as half of the total dorsoventral excursion (maximum–minimum). Frequency (Hz) was calculated as the number of fin beats per second. Wavespeed (mm s^{-1}) was measured as the distance between points 3 and 8 on the fin margin (Fig. 2) divided by the time required by the wave to travel that distance. Body angle (deg), the angle between the fish body and the flow, was measured using the three-dimensional distance between the x, y and z coordinates of the eye and the midpoint of the skate vertebral column (points 2 and 7, respectively; Fig. 2). Fin curvature (κ) during upstroke and

Journal of Experimental Biology (2017) 220, 705-712 doi:10.1242/jeb.148767

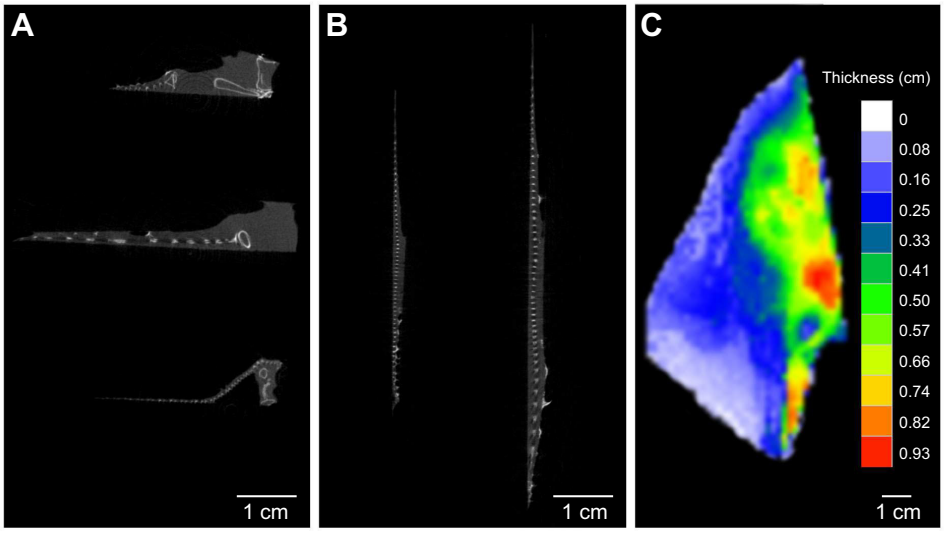

Fig. 1. Thickness of the left pectoral fin of a little skate, *Leucoraja erinacea*. Slices from a micro-CT scan of the left pectoral wing of a little skate, showing that thickness of the wing (A) decreases at three chordwise intervals, from anterior to posterior, and (B) increases at two spanwise intervals from distal to proximal. White regions indicate calcified cartilage, while light gray color represents skin and muscle tissue. (C) Map of pectoral wing thickness over the entire semi-disc.

downstroke was determined both chordwise and transversally at the distal margin of the fin (Blevins and Lauder, 2012; Standen and Lauder, 2005; Taft et al., 2008) using the equation $\kappa=|d\mathbf{T}/ds|$, where s is the arc length of a curve connecting all three points in the transect and $\mathbf{T}$ is the unit tangent vector of that curve.

Statistical analysis

We analyzed three fin beats from each individual (n=3) at the two speeds, for a total of 18 sequences. A two-way ANOVA, with speed and individual skate as factors, was performed separately on all kinematic variables (amplitude, frequency, fin curvature, wavespeed, body angle) followed by a Tukey's test to analyze differences between means. Any interactions found between factors are reported below following the ANOVA results. All values are presented as means±s.e.m. and all analyses were performed in JMP Pro (version 11, SAS Institute, Cary, NC, USA).

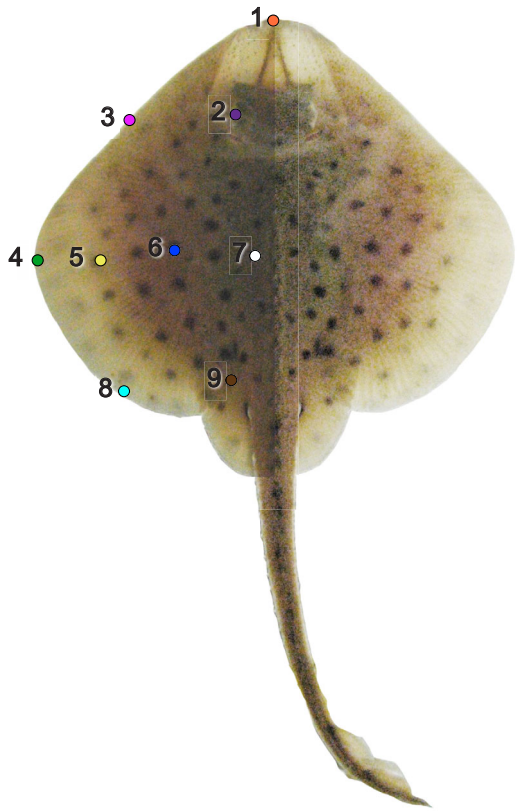

Fig. 2. Dorsal view of *Leucoraja erinacea*. A total of nine points were digitized every five frames (total of 50 frames s^{-1}) for each skate using natural markings (spots) on the left wing of the disc. Point colors and numbers match the data shown in Fig. 4.

RESULTS

Pectoral fin morphology

Measurements of the left pectoral fin show that thickness decreases to less than 1 mm toward the edge and posterior portion of the disc, while maximum thickness was measured at the midline of the skate at approximately 10 mm (Fig. 1). The anterior disc margin is thicker than the posterior margin (Fig. 1C). In the mediolateral direction, the thickness decrease is not uniform: there is a rapid initial decrease in disc thickness just lateral to the midline (Fig. 1A) followed by a thinning of the disc toward the lateral edge (Fig. 1B).

Swimming kinematics

Pectoral fin locomotion in little skates occurs via a propulsive wave passing from anterior to posterior along the fin (Fig. 3). Amplitude does not differ between speeds (two-way ANOVA, $F_{5,12}$=1.19, P=0.3; Figs 4, 6D), with the exception of one point in the posterior margin of the disc (point 8), where the pectoral fin forms a lobe at the posterior margin. Here, amplitude increases significantly at 2 BL s^{-1} (two-way ANOVA, $F_{5,12}$=3.71, P=0.03; Fig. 4), with a significant interaction between individual skate and speed (P=0.04). Higher amplitude closely matches areas of low thickness on the disc (Figs 1, 5) along both anteroposterior and mediolateral axes, with the highest value measured at the distal mid-disc point (Figs 4, 5). At maximum disc width (point 4), the wave has a mean amplitude of 13.8±0.8 mm, but reached a maximum amplitude of 20.5 mm (Fig. 5). However, this maximum amplitude does not significantly increase with speed (two-way ANOVA, $F_{5,12}$=1.19, P=0.3; Fig. 6D).

The skate disc also bends in the chordwise and transverse planes to create the propulsive wave (Fig. 3). We found no significant differences in chordwise curvature between upstroke (two-way ANOVA, $F_{3,14}$=0.99, P=0.4) and downstroke (two-way ANOVA, $F_{3,14}$=1.81, P=0.2) at either speed. However, we observed a sharp notch at the distal margin of the fin during downstroke at the higher

Journal of Experimental Biology (2017) 220, 705-712 doi:10.1242/jeb.148767

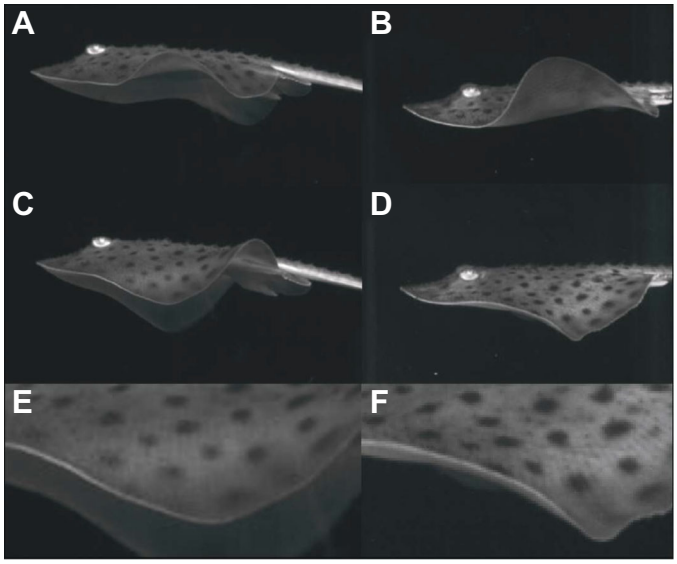

Fig. 3. Kinematics of skate locomotion. Lateral views from high-speed video frames of skate locomotion during the upstroke (A,B) and downstroke (C,D) at two speeds, 1 BL s^{-1} (A,C) and 2 BL s^{-1} (B,D). Close-up views of the fin margin during the downstroke at each speed are shown in E and F. Simultaneous dorsal view videos were obtained also so that each digitized point could be tracked in three dimensions, but these images are not shown here. Fin margin curvature differs considerably between the two speeds, with a pronounced sharp 'notch' evident at the higher speed downstroke (F). See the text (Discussion, Fin curvature and morphology) for further discussion.

speed (Fig. 3F) that travels posteriorly from mid-disc. This transversal curvature is significantly higher at 2 BL s^{-1} ($F_{1,4}$=8.29, P=0.04; Fig. 3E,F). We also observed a change in the curvature orientation in the mid-disc region as speed increased. At the slow swimming speed, the wing is curved in a concave upward direction during the downstroke, indicating that fluid pressure is deforming the wing, and curvature reverses during the upstroke to a concave downward configuration (Fig. 7, left panel). However, at the higher swimming speed (Fig. 7, right panel), wing conformation is concave downward during the downstroke. That is, the wing is curved into the direction of motion and in a direction that opposes fluid loading. During the upstroke, the fin is curved in the same direction of flow at both speeds (Figs 3A,B, 7).

Skates maintain a nearly horizontal orientation of the body during steady swimming with only small angular deviations from horizontal, but body angle decreases significantly from slightly positive at the slow swimming speed to slightly negative with increasing speed (two-way ANOVA, $F_{5,12}$=3.39, P=0.01; Fig. 6A). We found a significant interaction between skate and speed, where one individual showed a more pronounced difference in body angle between the two speeds (P=0.04). Frequency and wavespeed both increase significantly with swimming speed (P=0.02 and P=0.04, respectively; Fig. 6B,C).

DISCUSSION

Skate propulsion

Changes in kinematics, body orientation and shape of the pectoral fins provide evidence that little skates actively modulate their body position and wing waveform to control locomotion at different speeds. In particular, skates double their swimming speed by increasing frequency and wavespeed, and they adjust the body to a slightly negative angle at 2 BL s^{-1}. Amplitude also tends to increase slightly with speed, but the overall difference across the two speeds was not significant in the present study.

In addition, skates show complex deformations of the wing surface at higher speeds, including a previously undescribed 'notch' or sharp area of wing bending that travels posteriorly with the fin wave at the higher speed tested (Fig. 3F). Rosenberger (2001) tested another skate species, the clearnose skate, *Raja eglanteria*, at the same speeds but did not note the same feature nor is it apparent from the video frames published. Variation in fin deformation could arise from differences in wing thickness, morphology and shape. All of these variables change significantly in batoids (Fontanella et al., 2013; Schaefer and Summers, 2005). Most significantly, we measured patterns of mediolateral wing deformation that suggest a shift to active curvature control during the downstroke at the higher of the two swimming speeds. Mediolateral curvature of the wing at slower speeds appears to be a passive response to fluid loading, as in both the upstroke and downstroke we measured convex wing shape that reflects deformation as a result of the water–wing dynamic interaction. However, at the higher speed, and during the downstroke only, we measured concave mediolateral curvature with the wing cupped into the flow, strongly indicative of active muscular control of wing shape to resist forces exerted by the water on the wing.

We also note that the areas of reduced thickness on the expanded pectoral fins overlap with the peaks in amplitude across the disc (Figs 1, 5). The posterior disc margin is especially thin (on the order of 100–300 µm), and even thinner than the anterior and lateral disc margins. Without active stiffening that results from contraction of intrinsic fin musculature, at higher flapping frequencies fluid forces experienced by the fin disc would necessarily bend the surface and reduce locomotor forces, as discussed in more detail below.

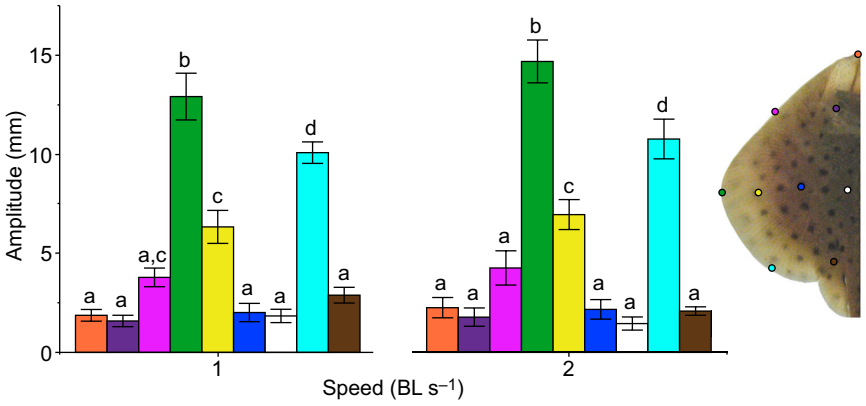

Fig. 4. Amplitude at different points on the skate disc. Amplitude (mm; mean±s.e.m.) at different points on the left wing of the little skate (n=3 individuals at each speed; n=18 fin-beat cycles total) as a function of speed (BL s^{-1}). Different letters represent significant differences in amplitude (two-way ANOVA followed by Tukey–Kramer multiple comparisons test, α=0.05). Bar colors match the markers shown on the skate wing to the right.

Journal of Experimental Biology (2017) 220, 705-712 doi:10.1242/jeb.148767

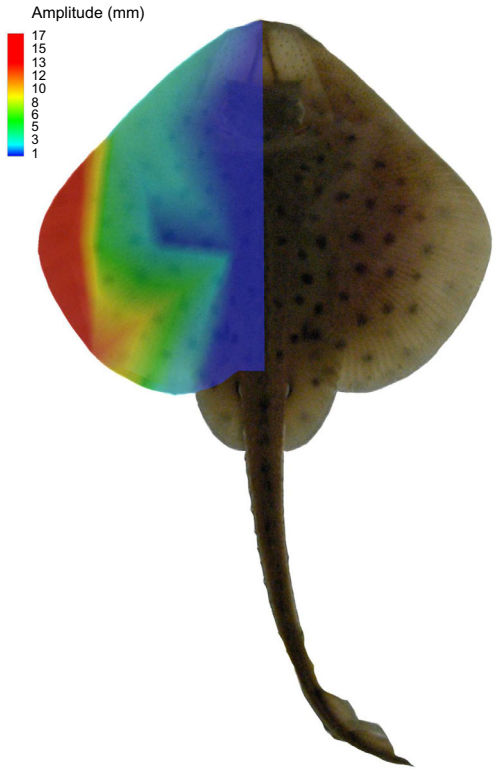

Fig. 5. Maximum amplitude of three-dimensional excursion across the skate disc. Maximum amplitude (mm) measured across the left wing of one individual little skate (here, we show skate 1 at 2 BL s^{-1}) closely matches areas of low thickness (Fig. 1C).

Comparison with other batoids

Batoids differ significantly from each other in their kinematics. The little skate is placed in the continuum between oscillators and undulators, and exhibits fewer 'extreme' or specialized features seen in benthic batoids, such as the freshwater stingray. As speed increases, little skates and freshwater stingrays show common features of wing kinematics which include increases in frequency and wavespeed, as well as non-significant changes in amplitude. Frequency modulation of disc motion appears to be the dominant mode of generating increased thrust in both species. Mean frequency is intermediate in little skate when compared with the highest value measured in the Atlantic guitarfish, *Rhinobatos lentiginosus* (4.2 Hz), and the lowest measured in the pelagic stingray, *Pteroplatytrygon violacea* (0.78 Hz), across a similar range of speeds (Rosenberger, 2001). Frequency in the freshwater stingray increases from approximately 2.5 to 3.8 Hz with speed (from 1.5 to 2.5 BL s^{-1}). In the little skate, mean frequency increased from approximately 1.66 to 2.11 Hz at the higher speed. Our values more closely approximate those measured for another rajiform, the clearnose skate, that showed a minimum and maximum frequency of approximately 1.38 and 2.07 Hz, respectively (Rosenberger, 2001). The differences observed across batoids underline the variation along a continuum in lifestyle and locomotor mode. Batoids that have high fin-beat frequency and low amplitude are considered benthic and they are tuned for maneuverability and slow swimming. In contrast, pelagic stingrays have a more oscillatory mode that enables long-distance translocations. Intermediate species, such as skates, have less undulatory fins, which allow for quick escapes. However, the low amplitude seen in skates and the fairly round disc of *L. erinacea* in particular are traits that limit the performance during steady swimming, especially at speeds beyond cruising. It is possible, however, to observe significant differences in skate pectoral fin locomotion, as this group presents species with a range of different shaped wings, from round to rhomboidal (McEachran and Dunn, 1998).

Little skates maintain a fairly horizontal body position during swimming, and similarly to other elasmobranch species, at low speeds they angle their body to generate lift (Rosenberger, 2001; Rosenblum et al., 2011; Wilga and Lauder, 2000). At the higher speed, however, little skates assume a slightly negative body angle, albeit this is not significantly different than an angle of 0 deg. A slightly negative body angle may allow skates to save energy at high speeds. In fact, in a study on the Japanese flounder, *Paralichthys olivaceus*, Kawabe et al. (2004) found that the fish would assume a

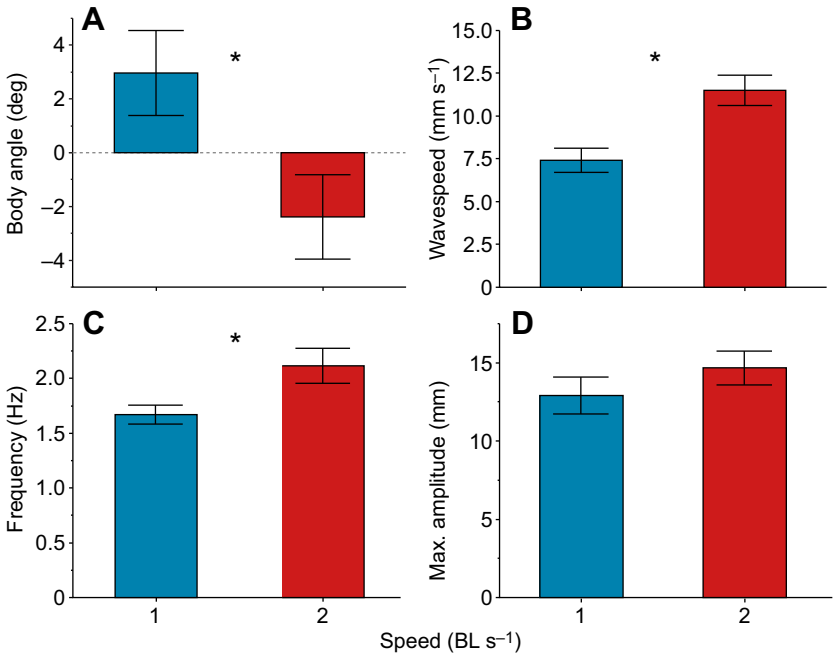

Fig. 6. Kinematic variables measured on the disc of little skates swimming at two speeds. Mean values for (A) body angle (deg), (B) wavespeed (mm s^{-1}), (C) frequency (Hz) and (D) maximum amplitude (mm) at two speeds, 1 and 2 BL s^{-1} (blue and red, respectively). Asterisks indicate significant differences between tested speeds (n=3 individuals; two-way ANOVA, followed by a Tukey–Kramer multiple comparisons test, α=0.05).

Journal of Experimental Biology (2017) 220, 705-712 doi:10.1242/jeb.148767

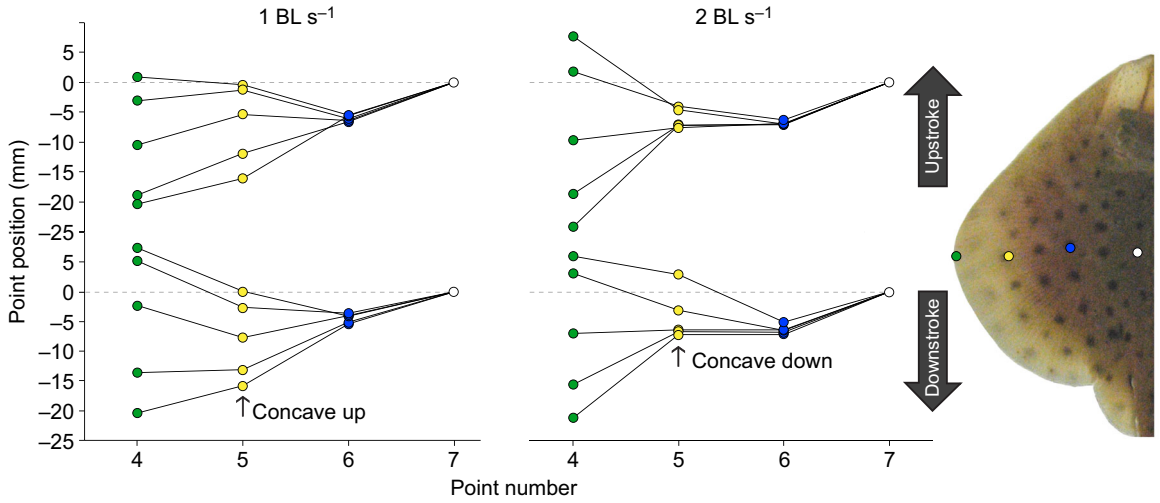

Fig. 7. Pattern of chordwise curvature on the wing during locomotion. Fin conformation at the mid-disc mediolateral position (markers shown on the skate wing to the right) during upstroke and downstroke, at two speeds. Thick arrows indicate direction of movement. Curvature calculations from these data are discussed in the text (Discussion, Fin curvature and morphology). Note that during the later stages of the downstroke at 2 BL s^{-1}, the wing is concave into the direction of motion, indicating active control of wing shape.

negative body angle at higher speeds to 'glide' and therefore decrease oxygen consumption. Although skates were not gliding at high speeds, it is possible that the negative (although slight) body angle may allow the fish to partially compensate for the unsustainable costs of locomotion beyond the optimal speed, because of increased fin-beat frequency and active stiffening of the wings.

Although locomotor behavior places the little skate within the undulatory benthic batoids, these new data suggest that there is much more diversity within each category than previously thought. Long and Nipper (1996) suggested that much of the source of variation comes from intraspecific differences in kinematics. In the present study, skates also present significant inter-individual variation in body angle, with one individual swimming markedly at a negative body angle at the higher speed tested. Rosenberger (2001) captured some locomotory diversity in her study on eight batoids, but a three-dimensional analysis of kinematics is necessary to describe patterns of curvature across the wing surface (Lauder and Di Santo, 2015). Such data indeed show some considerable differences between the little skate and the freshwater stingray (Blevins and Lauder, 2012). In particular, Blevins and Lauder (2012) noted that the lateral disc margin (but not the entire disc surface) could show a 'cupping' configuration where the margin bends actively during undulatory movement in the same direction as wing motion. This behavior of the disc surface was never observed in little skates. In addition, in the freshwater stingray, no differences in disc curvature on average were observed as speed increased from 1.5 to 2.5 BL s^{-1}. In contrast, little skates showed substantial changes in mediolateral disc curvature during the downstroke as speed increased, from a concave-up to a concave-down configuration, and we suggest that activation of intrinsic disc musculature curves the disc surface into the direction of downstroke motion.

Fin curvature and morphology

As speed increases, little skates alter the shape and curvature of the disc. Low-aspect-ratio discs, such as those of benthic batoids, typically have poor performance when compared with pelagic rays, because of induced drag (Fontanella et al., 2013; Lauder and Di Santo, 2015). Little skates change three-dimensional wing conformation and wavespeed perhaps because of the necessity to increase thrust as swimming speed increases, and consequently, the need for wing surface stiffening rises. At 2 BL s^{-1}, we observed a 'notch' or localized area of high curvature (Fig. 3F) on the lateral margin of the wing that travels throughout the fin-beat cycle from mid-disc margin to posterior. This localized region of high curvature may function to control how water flows over the fin edge and to increase thrust by directing more water posteriorly, a hypothesis that needs to be tested by quantifying water flow over the disc using particle image velocimetry (also see Lauder and Di Santo, 2015). Perhaps because the fin is so thin in the distal margin (Fig. 1), creating a notch will also increase effective wing thickness by increasing resistance to bending in the horizontal plane. By creating a sharp angle, the skate wing introduces a transversal arch that could represent an adaptation to achieve stiffness without adding mass (Dias et al., 2015).

In the little skate, wing curvature patterns differ at the two speeds between upstroke and downstroke. During upstroke, the fin assumes a curvature that we would expect from a passively flexible fin, with the edge of the fin bending away from the direction of overall fin motion in response to induced fluid pressure (Blevins and Lauder, 2012, 2013). If pectoral fin kinematics were simply the result of external fluid loading occurring as the fin is moved down against the fluid, then the fin margin would be expected to be curved upward. We observed this configuration of the fin margin at both speeds, as the fin margin was pushed in against the direction of flow. However, during downstroke, at the higher swimming speed, little skates actively cup their wing into the direction of motion. Active cupping to resist fluid loading is a phenomenon that has been observed in teleost fish pectoral fins (Lauder et al., 2006) and examined in robotic models of fin function (Esposito et al., 2012), where it was shown experimentally that cupping into the flow increases thrust. In addition, the bilaminar structure of fin rays in ray-finned fishes (Alben et al., 2007) has, as one function, the ability to actively generate curvature into oncoming flow and thus resist fluid loading.

When bending of the whole wing disc is analyzed, it is clear that while the whole fin may appear to undulate in lateral view (Rosenberger, 2001; Rosenberger and Westneat, 1999), only the

mid and posterior edge are actually experiencing significant bending (Blevins, 2012; Blevins and Lauder, 2012), and the disc thus has an anterior stabilized region with relatively little movement that experiences free-stream flow. If skates can use passive stiffening of the anterior edge of the fin while creating undulation on the posterior half of the disc, they could minimize energy costs during swimming at their preferred speed where they incur minimum locomotor costs, as observed in a previous energetic study (Di Santo and Kenaley, 2016). Conversely, at high speeds, benthic batoids need to actively engage more wing margin area as they propel through water, and this mechanism could limit their upper swimming capacity, a limitation not observed in mobuliform swimming (Fontanella et al., 2013; Lauder and Di Santo, 2015; Parson et al., 2011). We observed that at higher swimming speeds little skates generate active wing curvature that may function to both increase thrust and reduce fluid-induced deformation of the thin wing. This suggests that the recruitment of additional intrinsic wing musculature at high swimming speeds is necessary. Such additional muscle activity is also likely to increase the cost of transport and may render high-speed prolonged swimming in little skates especially energetically prohibitive, a conclusion also supported by recent studies of locomotor costs in skates (Di Santo, 2016; Di Santo and Kenaley, 2016).

Conclusions

The great majority of benthic batoids use their pectoral fins to swim in the water column. Work on batoid locomotion is scarce and limited to two-dimensional analyses, with the exception of the present study and a previous analysis of a freshwater species (Blevins and Lauder, 2012). The present study provides evidence that three-dimensional analyses of locomotor behavior, focused on patterns of pectoral wing deformation, can reveal shifts in configurations of fin use that suggest active stiffening of the fin at higher swimming speeds. In this species, such stiffening results in a sharp notch at the margin of the wing that travels from anterior to posterior with the propulsive wave. In addition, at higher speed, skates assume a slight negative body angle and enhance thrust by increasing wavespeed and fin-beat frequency, but not amplitude. Coupled with studies of pectoral morphology and previous analyses of locomotor energetics, we suggest that the relatively high cost of transport exhibited by little skates above their preferred swimming speed might result from the need to recruit additional musculature to actively stiffen the wing and generate increased thrust.

Acknowledgements

We thank members of the Lauder lab for assistance with fish care and discussions on fish locomotion. Thanks to Chris Kenaley for help with CT scanning and preparation of Fig. 1.

Competing interests

The authors declare no competing or financial interests.

Author contributions

V.D.S. and E.L.B. gathered the video data with assistance from G.V.L. V.D.S. analyzed the data, prepared the figures, and wrote the first draft of the manuscript. E.L.B. and G.V.L. contributed to subsequent manuscript drafts. All authors contributed to interpreting the results and presentation in the manuscript.

Funding

This work was supported by the National Science Foundation [grant EFRI-0938043] and funds from Harvard University.

Supplementary information

Supplementary information available online at
http://jeb.biologists.org/lookup/doi/10.1242/jeb.148767.supplemental

References

Alben, S., Madden, P. G. and Lauder, G. V. (2007). The mechanics of active fin-shape control in ray-finned fishes. *J. R. Soc. Inter.* **4**, 243-256.

Aschliman, N. C., Nishida, M., Miya, M., Inoue, J. G., Rosana, K. M. and Naylor, G. J. P. (2012). Body plan convergence in the evolution of skates and rays (Chondrichthyes: Batoidea). *Mol. Phylogenet. Evol.* **63**, 28-42.

Blevins, E. L. (2012). Undulatory locomotion in freshwater stingray *Potamotrygon orbignyi*: kinematics, pectoral fin morphology, and ground effects on rajiform swimming. *Doctoral dissertation*, Harvard University.

Blevins, E. L. and Lauder, G. V. (2012). Rajiform locomotion: three-dimensional kinematics of the pectoral fin surface during swimming in the freshwater stingray *Potamotrygon orbignyi*. *J. Exp. Biol.* **215**, 3231-3241.

Blevins, E. L. and Lauder, G. V. (2013). Swimming near the substrate: a simple robotic model of stingray locomotion. *Bioinspir. Biomim.* **8**, 016005.

Cloitre, A., Subramaniam, V., Patrikalakis, N. and Y Alvarado, P. V. (2012). Design and control of a field deployable batoid robot. In *Biomedical Robotics and Biomechatronics (BioRob)*, 2012 4th IEEE RAS & EMBS International Conference on Biomedical Robotics and Biomechatronics, Rome, Italy, 24-27 June 2012, pp. 707-712. IEEE.

Daniel, T. L. (1988). Forward flapping flight from flexible fins. *Can. J. Zool.* **66**, 630-638.

Dewey, P. A., Carriou, A. and Smits, A. J. (2012). On the relationship between efficiency and wake structure of a batoid-inspired oscillating fin. *J. Fluid Mech.* **691**, 245-266.

Di Santo, V. (2016). Intraspecific variation in physiological performance of a benthic elasmobranch challenged by ocean acidification and warming. *J. Exp. Biol.* **219**, 1725-1733.

Di Santo, V. and Kenaley, C. P. (2016). Skating by: low energetic costs of swimming in a batoid fish. *J. Exp. Biol.* **219**, 1804-1807.

Dias, M. A., Singh, D. K., Bandi, M. M., Venkadesan, M. and Mandre, S. (2015). Role of the tranverse arch in stiffness of the human foot. *APS Meeting Abstracts* **1**, 47003.

Donley, J. M. and Shadwick, R. E. (2003). Steady swimming muscle dynamics in the leopard shark *Triakis semifasciata*. *J. Exp. Biol.* **206**, 1117-1126.

Esposito, C. J., Tangorra, J. L., Flammang, B. E. and Lauder, G. V. (2012). A robotic fish caudal fin: effects of stiffness and motor program on locomotor performance. *J. Exp. Biol.* **215**, 56-67.

Fish, F. E., Schreiber, C. M., Moored, K. W., Liu, G., Dong, H. and Bart-Smith, H. (2016). Hydrodynamic performance of aquatic flapping: efficiency of underwater flight in the manta. *Aerospace* **3**, 20.

Flammang, B. E. (2010). Functional morphology of the radialis muscle in shark tails. *J. Morphol.* **271**, 340-352.

Fontanella, J. E., Fish, F. E., Barchi, E. I., Campbell-Malone, R., Nichols, R. H., DiNenno, N. K. and Beneski, J. T. (2013). Two- and three-dimensional geometries of batoids in relation to locomotor mode. *J. Exp. Mar. Biol. Ecol.* **446**, 273-281.

Franklin, O., Palmer, C. and Dyke, G. (2014). Pectoral fin morphology of batoid fishes (Chondrichthyes: Batoidea): explaining phylogenetic variation with geometric morphometrics. *J. Morphol.* **275**, 1173-1186.

Hedrick, T. L. (2008). Software techniques for two- and three-dimensional kinematic measurements of biological and biomimetic systems. *Bioinspir. Biomim.* **3**, 034001.

Kawabe, R., Naito, Y., Sato, K., Miyashita, K. and Yamashita, N. (2004). Direct measurement of the swimming speed, tailbeat, and body angle of Japanese flounder (*Paralichthys olivaceus*). *ICES J. Mar. Sci.* **61**, 1080-1087.

Koester, D. M. and Spirito, C. P. (2003). Punting: an unusual mode of locomotion in the little skate, *Leucoraja erinacea* (Chondrichthyes: Rajidae). *Copeia* **2003**, 553-561.

Krishnamurthy, P., Khorrami, F., De Leeuw, J., Porter, M. E., Livingston, K. and Long, J. H. (2010). An electric ray inspired biomimetic autonomous underwater vehicle. In Proceedings of the 2010 American Control Conference, 5224-5229.

Lauder, G. V. (2015). Fish locomotion: recent advances and new directions. *Annu. Rev. Mar. Sci.* **7**, 521-545.

Lauder, G. V. and Di Santo, V. (2015). Swimming mechanics and energetics of elasmobranch fishes. *Fish Physiol.* **34**, 219-253.

Lauder, G. V. and Jayne, B. C. (1996). Pectoral fin locomotion in fishes: testing drag-based models using three-dimensional kinematics. *Am. Zool.* **36**, 567-581.

Lauder, G. V., Madden, P. G. A., Mittal, R., Dong, H. and Bozkurttas, M. (2006). Locomotion with flexible propulsors: I. Experimental analysis of pectoral fin swimming in sunfish. *Bioinspir. Biomim.* **1**, S25-S34.

Long, J. H. and Nipper, K. S. (1996). The importance of body stiffness in undulatory propulsion. *Am. Zool.* **36**, 678-694.

Long, J. H., Krenitsky, N. M., Roberts, S. F., Hirokawa, J., de Leeuw, J. and Porter, M. E. (2011). Testing biomimetic structures in bioinspired robots: how vertebrae control the stiffness of the body and the behavior of fish-like swimmers. *Int. Comp. Biol.* **51**, 158-175.

Macesic, L. J. and Kajiura, S. M. (2010). Comparative punting kinematics and pelvic fin musculature of benthic batoids. *J. Morphol.* **271**, 1219-1228.

Macesic, L. J. and Summers, A. P. (2012). Flexural stiffness and composition of the batoid propterygium as predictors of punting ability. *J. Exp. Biol.* **215**, 2003-2012.
Macesic, L. J., Mulvaney, D. and Blevins, E. L. (2013). Synchronized swimming: coordination of pelvic and pectoral fins during augmented punting by the freshwater stingray *Potamotrygon orbignyi*. *Zoology* **116**, 144-150.
McEachran, J. D. and Dunn, K. A. (1998). Phylogenetic analysis of skates, a morphologically conservative clade of elasmobranchs (Chondrichthyes: Rajidae). *Copeia* **1998**, 271-290.
Moored, K. W., Dewey, P. A., Leftwich, M. C., Bart-Smith, H. and Smits, A. J. (2011a). Bioinspired propulsion mechanisms based on manta ray locomotion. *Marine Tech. Soc. J.* **45**, 110-118.
Moored, K. W., Fish, F. E., Kemp, T. H. and Bart-Smith, H. (2011b). Batoid fishes: inspiration for the next generation of underwater robots. *Marine Tech. Soc. J.* **45**, 99-109.
Nakamura, T., Klomp, J., Pieretti, J., Schneider, I., Gehrke, A. R. and Shubin, N. H. (2015). Molecular mechanisms underlying the exceptional adaptations of batoid fins. *Proc. Natl. Acad. Sci. USA* **112**, 15940-15945.
Park, S.-J., Gazzola, M., Park, K. S., Park, S., Di Santo, V., Blevins, E. L., Lind, J. U., Campbell, P. H., Dauth, S., Capulli, A. K. et al. (2016). Phototactic guidance of a tissue-engineered soft-robotic ray. *Science* **353**, 158-162.
Parson, J. M., Fish, F. E. and Nicastro, A. J. (2011). Turning performance of batoids: limitations of a rigid body. *J. Exp. Mar. Biol. Ecol.* **402**, 12-18.
Porter, M. E., Roque, C. M. and Long, J. H., Jr. (2011). Swimming fundamentals: turning performance of leopard sharks (*Triakis semifasciata*) is predicted by body shape and postural reconfiguration. *Zoology* **114**, 348-359.
Root, R. G., Courtland, H.-W., Shepherd, W. and Long, J. H. (2007). Flapping flexible fish. *Exp. Fluids* **43**, 779-797.
Rosenberger, L. J. (2001). Pectoral fin locomotion in batoid fishes: undulation versus oscillation. *J. Exp. Biol.* **204**, 379-394.
Rosenberger, L. J. and Westneat, M. W. (1999). Functional morphology of undulatory pectoral fin locomotion in the stingray *Taeniura lymma* (Chondrichthyes: Dasyatidae). *J. Exp. Biol.* **202**, 3523-3539.
Rosenblum, H. G., Long, J. H. and Porter, M. E. (2011). Sink and swim: kinematic evidence for lifting-body mechanisms in negatively buoyant electric rays *Narcine brasiliensis*. *J. Exp. Biol.* **214**, 2935-2948.
Schaefer, J. T. and Summers, A. P. (2005). Batoid wing skeletal structure: novel morphologies, mechanical implications, and phylogenetic patterns. *J. Morphol.* **264**, 298-313.
Standen, E. M. and Lauder, G. V. (2005). Dorsal and anal fin function in bluegill sunfish *Lepomis macrochirus*: three-dimensional kinematics during propulsion and maneuvering. *J. Exp. Biol.* **208**, 2753-2763.
Taft, N. K., Lauder, G. V. and Madden, P. G. A. (2008). Functional regionalization of the pectoral fin of the benthic longhorn sculpin during station holding and swimming. *J. Zool.* **276**, 159-167.
Tytell, E. D. and Lauder, G. V. (2004). The hydrodynamics of eel swimming. *J. Exp. Biol.* **207**, 1825-1841.
Tytell, E. D., Hsu, C.-Y., Williams, T. L., Cohen, A. H. and Fauci, L. J. (2010). Interactions between internal forces, body stiffness, and fluid environment in a neuromechanical model of lamprey swimming. *Proc. Nat. Acad. Sci. USA* **107**, 19832-19837.
Tytell, E. D., Hsu, C.-Y. and Fauci, L. J. (2014). The role of mechanical resonance in the neural control of swimming in fishes. *Zoology* **117**, 48-56.
van Ginneken, V., Antonissen, E., Müller, U. K., Booms, R., Eding, E., Verreth, J. and van den Thillart, G. (2005). Eel migration to the Sargasso: remarkably high swimming efficiency and low energy costs. *J. Exp. Biol.* **208**, 1329-1335.
Wilga, C. D. and Lauder, G. V. (2000). Three-dimensional kinematics and wake structure of the pectoral fins during locomotion in leopard sharks *Triakis semifasciata*. *J. Exp. Biol.* **203**, 2261-2278.
Wilga, C. D. and Lauder, G. V. (2002). Function of the heterocercal tail in sharks: quantitative wake dynamics during steady horizontal swimming and vertical maneuvering. *J. Exp. Biol.* **205**, 2365-2374.

Journal of Experimental Biology

Movie S1. Little skate, *Leucoraja erinacea*, during steady swimming at 2 BL × s^{-1}. The sequence was recorded at 250 frames × s^{-1}.